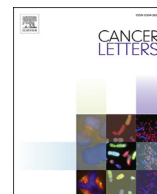




Contents lists available at ScienceDirect

Cancer Letters

journal homepage: www.elsevier.com/locate/canlet

Original Article

Multiparity activates interferon pathways in peritoneal adipose tissue and decreases susceptibility to ovarian cancer metastasis in a murine allograft model[☆]

Elizabeth A. Loughran^{a, c, d}, Ryan C. Phan^d, Annemarie K. Leonard^{a, d}, Laura Tarwater^d, Marwa Asem^{a, c, d}, Yueying Liu^g, Jing Yang^{a, d}, Yuliya Klymenko^{b, d}, Jeff Johnson^{a, d}, Zonggao Shi^d, Tyvette Hilliard^{a, d}, Marielle Blumenthaler^d, Matthew Leevy^{b, d}, Matthew J. Ravosa^{b, d, e, f}, M. Sharon Stack^{a, d, *}

^a Department of Chemistry and Biochemistry, University of Notre Dame, Notre Dame, IN, USA

^b Department of Biological Sciences, University of Notre Dame, Notre Dame, IN, USA

^c Integrated Biomedical Sciences Graduate Program, University of Notre Dame, Notre Dame, IN, USA

^d Harper Cancer Research Institute, University of Notre Dame, Notre Dame, IN, USA

^e Department of Aerospace and Mechanical Engineering, University of Notre Dame, Notre Dame, IN, USA

^f Department of Anthropology, University of Notre Dame, Notre Dame, IN, USA

^g University of Notre Dame, USA

ARTICLE INFO

Article history:

Received 1 August 2017

Received in revised form

19 September 2017

Accepted 21 September 2017

Keywords:

Ovarian cancer metastasis

Parity

Interferons (IFNs)

Murine age-matched model of parity

Adipose tissue

ABSTRACT

Ovarian cancer is the fifth leading cause of cancer deaths in U.S. women and the deadliest gynecologic malignancy. This lethality is largely due to the fact that most cases are diagnosed at metastatic stages of the disease when the prognosis is poor. Epidemiologic studies consistently demonstrate that parous women have a reduced risk of developing ovarian cancer, with a greater number of births affording greater protection; however little is known about the impact of parity on ovarian cancer metastasis. Here we report that multiparous mice are less susceptible to ovarian cancer metastasis in an age-matched syngeneic murine allograft model. Interferon pathways were found to be upregulated in healthy adipose tissue of multiparous mice, suggesting a possible mechanism for the multiparous-related protective effect against metastasis. This protective effect was found to be lost with age. Based on this work, future studies exploring therapeutic strategies which harness the multiparity-associated protective effect demonstrated here are warranted.

© 2017 Published by Elsevier B.V.

Introduction

The most fatal of gynecological cancers and the fifth leading cause of cancer-related deaths in U.S. women, ovarian cancer is usually diagnosed at metastatic stages of the disease, which contributes to poor prognoses [1]. It is commonly believed that ovarian cancer metastasizes uniquely when cells or multicellular

aggregates shed from the primary tumor, disseminate throughout the peritoneal cavity and form metastatic sites on peritoneal tissues [1]. Recent studies have also reported hematogenous metastasis in model systems, although metastatic homing to the ovary was reported by both authors [2,3].

Epidemiologic studies have repeatedly demonstrated that parous women, or women who have given birth, have a reduced risk of developing ovarian cancer, with more births providing a greater protective effect [4–10]. The European Prospective Investigation into Cancer and Nutrition revealed that parous women have a 29% lower risk of developing ovarian cancer and each pregnancy further reduces the risk by 8% [8]. While epidemiologic data on the parity status of ovarian cancer patients gives valuable information on cancer incidence, little data are available evaluating the impact of parity on metastasis. As metastatic disease is the cause of the vast

[☆] This work was supported by Grants R01CA109545 (MSS) and R01CA086984 (MSS) from the National Institutes of Health/National Cancer Institute; from the Leo and Anne Albert Charitable Trust (MSS); National Science Foundation Graduate Research Fellowship Program grant DGE-1313583 (EAL).

* Corresponding author. University of Notre Dame, Harper Cancer Research Institute, 1234 Notre Dame Ave., A200 Harper Hall, South Bend, IN 46617, USA.

E-mail address: sstack@nd.edu (M.S. Stack).

majority of ovarian cancer deaths, development of model systems with which to examine the relationship between parity and ovarian cancer metastasis is warranted.

In addition to epidemiologic data, a single study has reported the impact of parity on ovarian cancer metastasis in a murine model, comparing intraperitoneal metastasis of mouse ovarian surface epithelial (MOSE) cancer cells in C57Bl/6 nulliparous 5-month-olds to 12-month-old retired breeders [11]. The middle-aged parous animals developed significantly less tumor burden than the younger virgin animals and this resilience was attributed to parity-associated differences in the immune compositional profile in the omental fat band [11].

The purpose of our study was to investigate the role of specific parity number on ovarian cancer metastasis in an age-matched host. Using an age-matched murine model of parity and ovarian cancer metastasis, we found that multiparity, but not primiparity, reduces susceptibility to ovarian cancer metastasis in mature adult mice, but not in aged mice. Investigation of healthy non-tumor bearing periovarian adipose tissue from parity groups indicate that a multiparity-associated upregulation of interferon-stimulated genes (ISGs) may be responsible for reduction of metastasis to the gonadal adipose tissue in multiparous animals.

Materials and Methods

Murine parity model

C57Bl/6 female mice (Jackson Laboratories) were bred zero, one or three times beginning at 8 weeks of age to generate mice of three parity statuses: Para 0 (nulliparous, P0), Para 1 (primiparous, P1), and Para 3 (multiparous, P3) (Fig. 1A). Mice of differing parity statuses were age-matched within experiments. All pregnancies resulting in the birth of pups were counted towards parity number. For the murine aging parity model, aged-matched P0, P1 and P3 mice were allowed to age until 20.5 months of age prior to tumor study. This experimental time point was chosen based on research on mouse-human lifespan equivalencies carried out by the Harrison Lab at Jackson laboratories and corresponds to women over the age of 60 [12]. All animal procedures were carried out according to the regulations of the Institutional Animal Care and Use Committee (IACUC) at The University of Notre Dame.

Murine allograft model of ovarian cancer metastasis

The MOSE ID8 ovarian cancer cell line, syngeneic to C57Bl/6 mice, used in allograft studies, was tagged with red fluorescent protein (RFP) and maintained as previously described [13,14]. As ovarian cancers metastasize mainly by direct extension and shedding from the primary tumor into the peritoneal cavity, an intraperitoneal (IP) injection model was used to assess metastatic dissemination. This model captures key events in metastasis including peritoneal adhesion, submesothelial anchoring and proliferation, but does not probe the initial event of metastatic cell dissociation from the primary tumor. To model the dissemination and colonization events of ovarian cancer metastasis, ID8 RFP-tagged cells (10^7) were injected IP into age-matched 5.5-month-old P0, P1, and P3 mice. Parous mice were not injected with tumor cells until pups were completely weaned. To monitor tumor progression beginning at 5 weeks post injection, the mice were imaged once a week, under isoflurane anesthesia, using the Bruker Xtreme In Vivo Imaging system. Additionally, mice were observed for signs of lethargy or ascites accumulation. A parallel experiment was carried out in age-matched 20-month-old P0, P1, and P3 mice. The mice were imaged live at 6 weeks post injection and sacrificed for dissection around 8 weeks post injection following IACUC protocol. The ventral skin was pulled away and the peritoneal cavity was exposed with incisions down the midline and the sides of the ventral parietal peritoneum. The abdominal organs were scanned *in situ* as previously described using the Bruker Xtreme In Vivo Imaging system [14,15]. The organs were removed and imaged *ex vivo*. The abdominal and organ images underwent spectral unmixing using the Bruker Multispectral software as previously described [15]. Using ImageJ, tumor burden in the abdominal and organ images was analyzed by calculating the tumor area and the intensity of the RFP signal (Raw Integrated Density). In the case of abdominal images, the measurements were corrected using the adjusted body weight of the mouse to control for differences between animals using the equation: adjusted body weight = $\text{weight}^{2/3}$. Either the area of the organs or the adjusted weight of the organs ($\text{weight}^{2/3}$) was used to control for animal-to-animal differences in organ size [15]. Statistical analysis was carried out using a parametric ANOVA (SYSTAT version 11) when $n = 10$, or the nonparametric Mann-Whitney *U* Test when $n = 5$ (analysis carried out in R [16]). A *p*-value cutoff of 0.05 was counted as statistically significant and $p < 0.1$ was also noted. After imaging, organs were fixed in 10% formalin and processed for paraffin embedding for histological analysis. After deparaffinization,

tissue sections were stained with SelectTech hematoxylin and eosin (H&E) staining system according to Leica's H&E protocol.

RNA isolation from gonadal adipose tissue and RNAseq analysis

Gonadal adipose tissue (up to 100 mg) from age-matched P0, P1, and P3 mice (between 6.3 and 6.9 months of age) was removed, placed directly into QIAzol Lysis Reagent (RNeasy® Plus Universal Kit), and homogenized (OMNI International, TH Tissue Homogenizer). RNA was isolated using the RNeasy® Plus Universal Kit according to the manufacturer's protocol. RNA was eluted from the RNeasy kit spin column with RNAase-free water (Ambion, Nuclease-free water, Not DEPC-Treated AM9930) and stored at -80°C until preparation for RNAseq or cDNA synthesis for qRT-PCR.

The Notre Dame Genomics and Bioinformatics Core Facility carried out the genomic and bioinformatic analyses detailed in the following sections. Initial RNA concentration was determined using the Qubit 2.0 Fluorometer and RNA High Sensitivity Assay (Life Technologies Corp., Carlsbad, CA). Total RNA integrity was assessed using the Agilent 2100 Bioanalyzer along with the RNA 6000 Pico Kit (Agilent Technologies, Santa Clara, CA). All samples had an RNA Integrity Number (RIN) value greater than or equal to 8. Libraries were constructed using the TruSeq RNA Sample Preparation Kit v2 set A and protocol companion (Illumina, Inc., San Diego, CA). Final library integrity and size distribution was assessed using the Agilent Bioanalyzer 2100 along with the DNA 7500 Assay (Agilent Technologies, Santa Clara, CA). The Qubit 2.0 Fluorometer along with the High Sensitivity DNA Assay (Life Technologies Corp.) was used to determine final library concentration. Libraries were normalized to 10 nM in buffer EB (Qiagen, Santa Clarita, CA) and combined together for multiplexing. Sequencing was conducted on three lanes of Illumina HiSeq2500 (University of New Hampshire) using 100bp paired-end reads. An average of 43 million paired-end reads were obtained per sample.

Bioinformatics

Raw sequences were trimmed of adapters with Trimmomatic [17], version 0.32, and assessed for quality with FastQC [18], version v0.11.2. Trimmed sequences were aligned to the Mus_musculus.GRCm38 Ensembl version of the mouse genome, using Mus_musculus.GRCm38.81 annotations [19], with TopHat2 [20], version 2.0.11.Linux_x86_64, using Bowtie 2 [21], version 2.2.2. Corresponding alignments were sorted with SAMtools [22], version 0.1.19. Read counts were generated with HTSeq-count [23], version 0.6.1, and were merged with a python script [24]. Subsequent statistics were completed in R [16], version 3.1.0, implementing the EdgeR library [25–28]. Gene names and GO terms were identified using the Ensemble version of BioMart [29]. Metacore pathway analysis was used to view pathways enriched in differentially expressed genes using a cutoff of $p = 0.05$.

Quantitative real-time PCR

RNA from periovarian adipose tissue was converted to cDNA using a QuantiTect® Reverse Transcription Kit (QIAGEN) according to the manufacturer's specifications. qRT-PCR reactions were set up using iTAQ™ Universal SYBER® Green Supermix (BIO-RAD) according to the manufacturer's specifications, using a StepOnePlus Real-Time PCR Thermal Cycler System (Applied Biosystems, StepOne Software V2.2.2). Primers, listed in Supplemental Table 1, were custom ordered from Integrated DNA Technologies (Coralville, Iowa). RSP13 and HPRT were used as endogenous controls to calculate ΔCt values. PCR thermal cycling conditions were as follows: 95°C for 10 min followed by 40 cycles of 95°C for 15s and 60°C for 60s. Biological replicates of $n = 4$ and three technical replicates were utilized for each experiment. The nonparametric Mann-Whitney *U* Test was selected to determine if ΔCt values of the young and aged samples were significantly different from each other (significance cutoff $p = 0.05$, $p < 0.1$ was also noted, analysis carried out in R [16]).

Results

Epidemiologic data support a link between parity and ovarian cancer incidence. However, the impact of parity on metastasis has not been evaluated in age-matched cohorts. To investigate the effect of parity on the final events in ovarian cancer metastasis (peritoneal seeding, anchoring and proliferation), 5.5-month aged-matched parity cohorts (P0, P1, and P3) were injected IP with ID8 RFP-tagged cells (10^7) (Fig. 1A). ID8 cells are a syngeneic MOSE cell line and hold the advantage of compatibility with mice bearing an intact immune system, unlike xenograft models. Mice were imaged under anesthesia at 5, 6, and 7 weeks post injection to monitor tumor progression (Supplemental Fig. 1). The live imaging data indicated that P3 mice had the least tumor burden among the parity groups. At 8 weeks post injection, mice were sacrificed and dissected. The abdominal cavity was exposed and the entire body

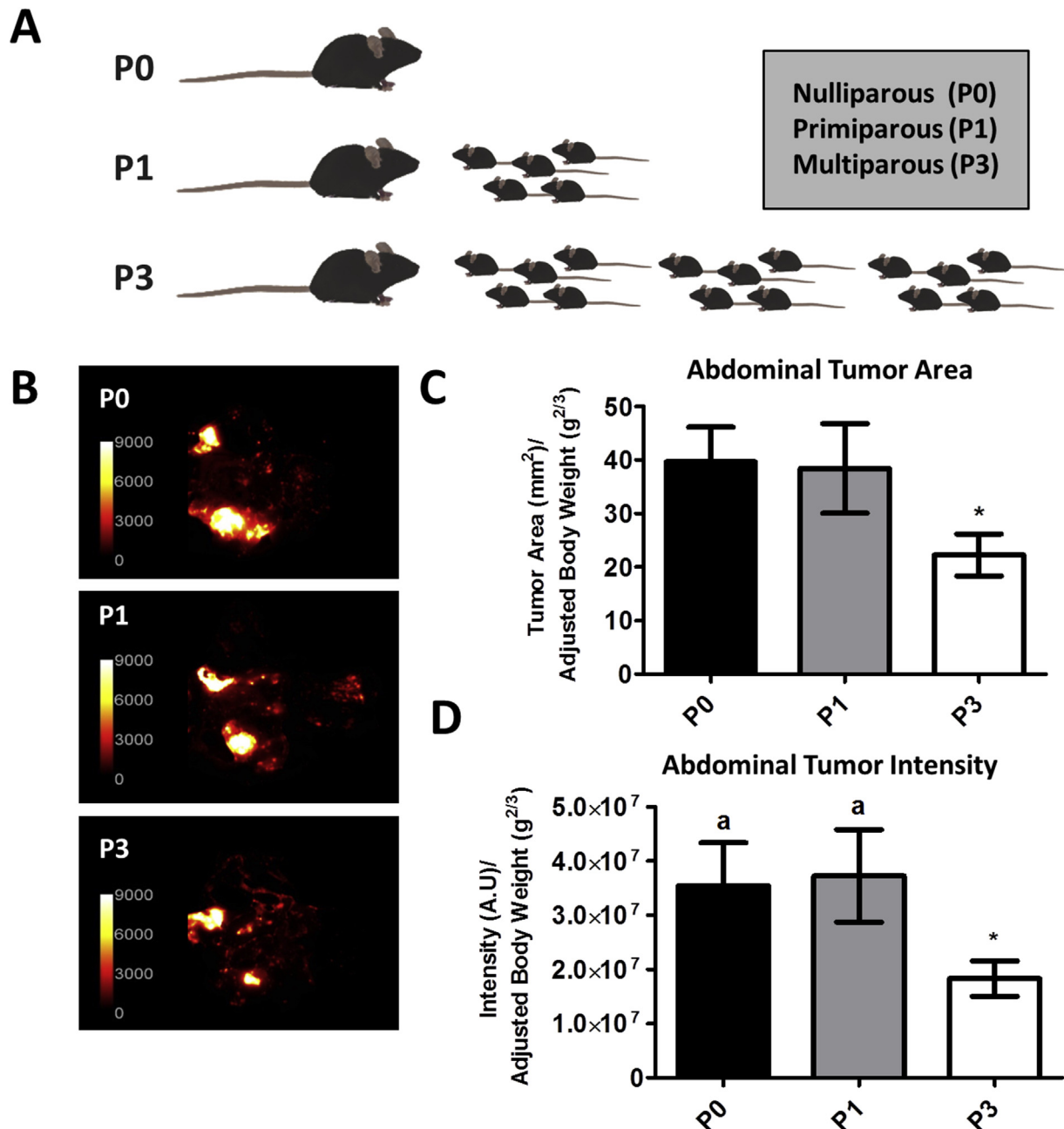


Fig. 1. Multiparity decreases metastatic burden. A. The C57Bl/6 parity mouse model. To investigate the role of parity in ovarian cancer metastasis, three parity statuses of C57Bl/6 mice were selected for this study. Nulliparous animals (P0) were not bred. Para 1 (P1) animals gave birth to 1 litter and Para 3 (P3) animals gave birth to 3 litters. The parous mice were bred beginning at 8 weeks of age. **B. Abdominal tumor burden *in situ*.** Mice were injected IP with 10^7 ID8 mouse ovarian cancer cells tagged with RFP. After sacrifice at 8 weeks post IP injection, the abdominal cavity was exposed and imaged. **C,D.** Tumor area and intensity, respectively, were quantified as described in Materials and Methods. Abdominal tumor area and abdominal tumor intensity were calculated by dividing either the tumor area or the tumor intensity by the scale-adjusted body weight of each mouse. N = 9, 10, 10 for P0, P1, P3, respectively. For Tumor Area, $p = 0.03$ for P0-P3 and $p = 0.1$ for P1-P3. For Tumor Intensity, $p = 0.05$ for P0-P3 and $p = 0.05$ for P1-P3.

was imaged *in situ*. The abdominal tumor area and the abdominal tumor intensity, parallel methods of analysis using ImageJ, consistently demonstrated that P3 mice develop significantly less tumor burden than P0 mice (Fig. 1B–D). Abdominal tumor area was therefore used for remaining analyses. Next, individual organs were dissected and imaged *ex vivo*. Quantitative analyses demonstrate that P3 mice have significantly less tumor burden in several tissues including the gonadal adipose tissue dissected from the left side of the uterus (FatL) and the periovarian adipose tissue, imaged with the ovaries and uterus attached (Fig. 2A and B). No significant difference was detected in the omentum. The organ tumor burden

analysis suggests that the difference in tumor burden in the gonadal adipose tissue appears to be driving the difference in overall abdominal tumor burden observed between parity groups (Figs. 1 and 2B). Following *ex vivo* imaging, tissues were processed for histology. H&E staining shows the periovarian adipose tissue surrounded by ID8 cells (Fig. 2C). Often there is a fibrosis layer in the ID8 cell: adipocyte border (arrows).

To explore why gonadal adipose tissue of P3 mice is less susceptible to metastatic seeding and growth, RNAseq was carried out on gonadal adipose RNA isolated from 4 healthy non-tumor bearing animals of each parity status (Supplemental Fig. 2). Three pairwise

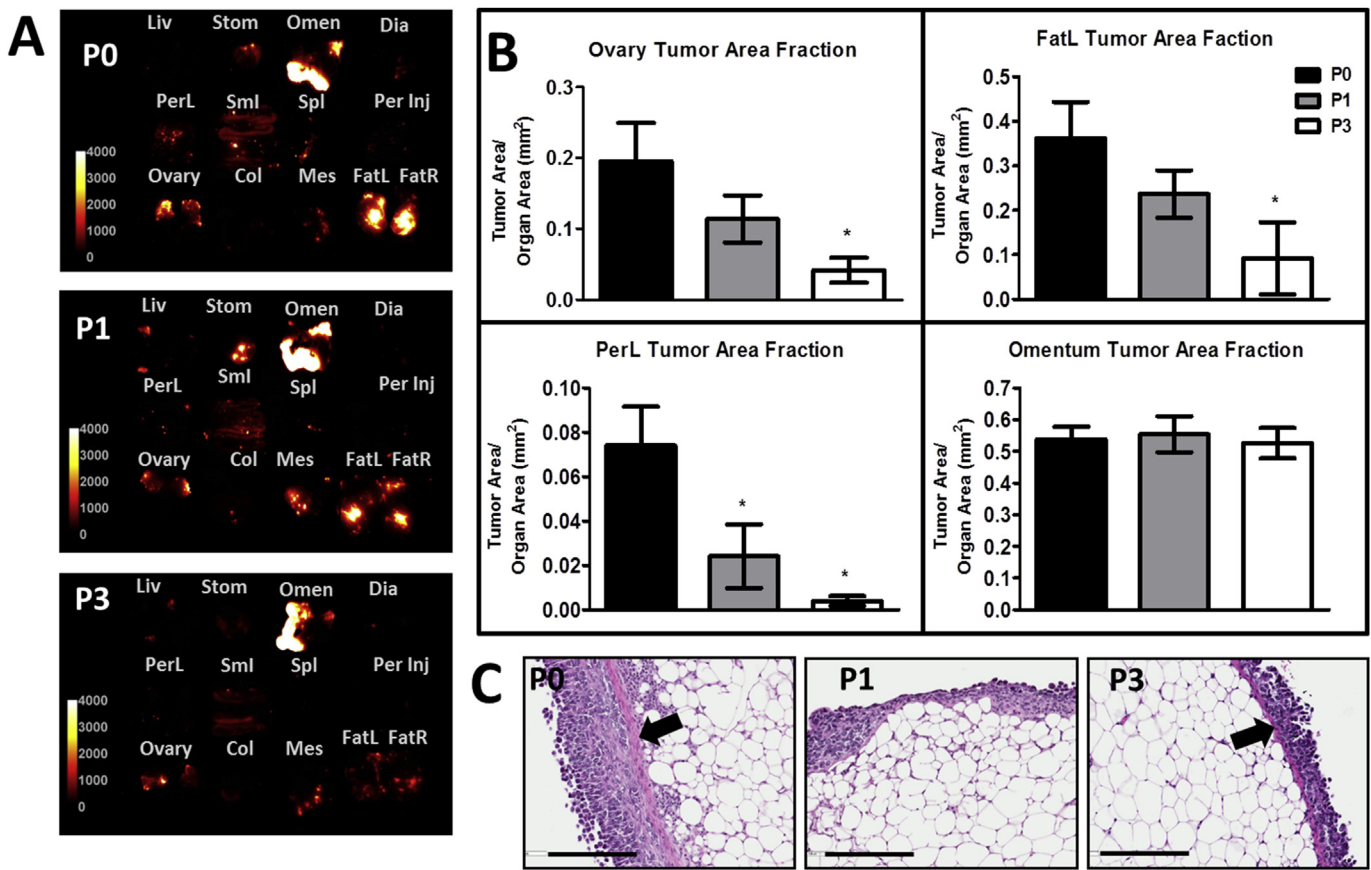


Fig. 2. Evaluation of organ-specific tumor burden in P0, P1, and P3 mice. A. Representative tumor burden images. Individual organs were dissected from the mouse peritoneal cavity and imaged. N = 9, 10, 10 for P0, P1, P3, respectively. Liv = liver, Stom = stomach, Omen = omentum/pancreas, Dia = diaphragm, PerL = parietal peritoneum left, Sml = small intestine, Spl = spleen, PerInj = parietal peritoneum injection side, Ovary = ovaries/uterus and periovarian adipose, Col = colon, Mes = mesentery, FatL = gonadal adipose tissue from the left of the uterus, FatR = gonadal adipose tissue from the right of the uterus. **B. Quantification of organ-specific tumor burden.** The Organ Area Fraction was calculated by dividing the tumor area by the organ area. Organs with significant differences between parity groups are shown, with the omentum as reference. For ovary, $p = 0.01$ P0-P3, $p = 0.07$ P1-P3; FatL, $p = 0.03$ P0-P3; PerL, $p = 0.04$ P0-P1, $p = 0.001$ P0-P3. **C. Representative H&E staining of the periovarian adipose tissue.** After imaging, the organs were fixed in 10% formalin and processed for histology. Scale bar equals 200 μ m. Arrows denote fibrosis layer.

comparisons were made with the resulting RNAseq data: P0 vs P1, P0 vs P3, and P1 vs P3 (Fig. 3A). Approximately 1600 genes were differentially expressed among the three comparisons and the parity groups displayed a unique expression signature (Fig. 3A). MetaCore™ pathway analysis revealed that among the pathways enriched in the dataset, an interferon (IFN) pathway was prominent (Fig. 3B, Supplemental Table 2). Specifically, IFN pathways appeared to be upregulated in P3 mice, as close to 22% of the upregulated genes overlapping in the P0 vs P3 and P1 vs P3 comparisons were IFN-related (Fig. 3A). Type I and type II IFNs have a variety of functions, including host defense, immunomodulation and anti-proliferative activity [30,31]. From the RNAseq data, several transcriptional regulators of IFNs or interferon-stimulated genes (ISGs) were chosen for validation by qRT-PCR based on expression levels (Table 1). Transcriptional regulators of IFNs included STAT1, an activator of both type I and II IFNs [30], IRF7, which has been dubbed the master regulator of type I IFN [32], and IRF1, an activator of type II IFN [33]. Validated ISGs included several guanylate-binding proteins (GBPs) [34], MX Dynamin Like GTPase 1 (Mx1, also known as Interferon-Inducible Protein P78) [31] and class II major histocompatibility complex transactivator (CIITA) [35] (Fig. 3B).

A recent study suggested that the protective effect of parity against developing ovarian cancer in women decreases with age [36]. To investigate if the reduced susceptibility to metastasis identified in the P3 adult mice (Fig. 1B–D) was retained in an aging

cohort, we carried out an additional ID8 allograft study with aged mice. In this cohort, 20.5-month-old age matched P0, P1, and P3 mice were injected IP with ID8 RFP-tagged cells (10^7). Unlike results observed in mature mice, live imaging suggested no difference between the groups at 6 weeks post injection (Supplemental Fig. 3). At 8 weeks post injection mice were sacrificed and imaged *in situ* and *ex vivo* (Fig. 4). No significant difference was found between the parity groups. These data suggest that the protective effect of multiparity against metastasis is not retained with aging. While the reasons for this may be distinct from those resulting in the reduced protective effect of parity against developing ovarian cancer [36], it is notable that our metastasis data follows a similar trend to epidemiologic data (Fig. 5).

Discussion

Parity is a well-established protective factor against ovarian cancer. Epidemiologic studies consistently report that women who have given birth are less likely to develop ovarian cancer [4–6,8–10]. This parity-associated protective effect increases with multiple births [8,9]. For decades, ovarian cancer researchers have been seeking to understand why parity reduces ovarian cancer risk and a number of theories have been proposed to explain this phenomenon. Among these theories is the incessant ovulation hypothesis, which maintains that ovulation contributes to the

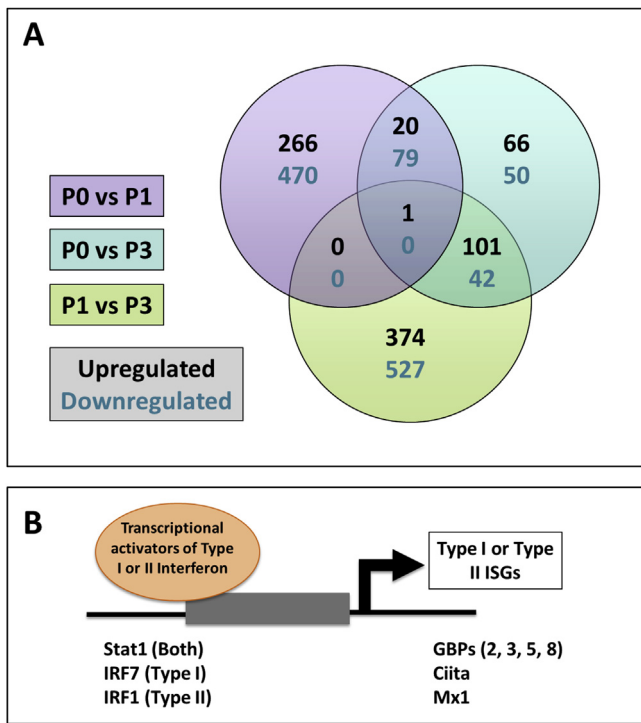


Fig. 3. RNASeq analysis of gonadal adipose tissue. **A.** Venn diagram representation of the upregulated and downregulated genes from RNAsequencing data for each pairwise comparison of parity groups. Gonadal adipose RNA of healthy non-tumor bearing mice ($n = 4$) from each parity group was isolated (Supplemental Fig. 2) and was subjected to RNA sequencing. This Venn diagram represents all genes with p -value less than 0.05. Each parity group comparison displayed a unique expression profile. **B.** Schematic of differentially expressed genes in interferon pathways. Metacore pathway analysis revealed enrichment of genes in IFN pathways. In this schematic, genes validated by qRT-PCR, which are IFN transcriptional activators or ISGs, are represented.

Table 1
qRT-PCR validation panel of interferon-related genes. The differential expression of IFN-related genes and several other prominent genes in the dataset was quantified using qRT-PCR, as described in Materials and Methods. Two normalizer genes, RSP13 and HPRT, were utilized and showed a similar trend. $N = 4$.

Gene	P1 vs P3 with Average Fold Change	RSP13 p-value	P1 vs P3 with Average Fold Change	HPRT p-value	P0 vs P3 with Average Fold Change	RSP13 p-value	P0 vs P3 with Average Fold Change	HPRT p-value
Ccr5	1.99	0.2			NS	NS		
CD274	NS	NS	NS	NS	NS	NS	NS	NS
Ciita	2.12	0.1143	2.15	0.02857	NS	NS	NS	NS
Clec4a1	1.86	0.2			NS	NS		
CXCL9	2.34	0.2	NS	NS	NS	NS	2.09	0.2
GBP11	3.4	0.1143	3.45	0.1143	2.66	0.1143	3.18	0.1143
GBP2	4.88	0.1143	4.95	0.05714	NS	NS	NS	NS
GBP2b	3.56	0.1143	3.61	0.1143	NS	NS	NS	NS
GBP3	5.25	0.1143	5.32	0.05714	NS	NS	2.88	0.1143
GBP5	2.28	0.05714	NS	NS	NS	NS	NS	NS
GBP7	2.51	0.1143	1.67	0.2	NS	NS	NS	NS
GBP8	4.41	0.1143	4.48	0.05714	NS	NS	NS	NS
H2-DMb1	1.98	0.2			NS	NS		
H2-K1	3.15	0.1143	3.2	0.1143	NS	NS	2.20	0.2
H2-Q6	NS	NS			NS	NS		
Ilgp1	4.72	0.2	4.79	0.1143	2.91	0.2	3.48	0.1143
IRF1	2.18	0.05714	2.21	0.05714	NS	NS	NS	NS
IRF7	1.45	0.1143	NS	0.1143	1.58	0.05714	1.9	0.05714
LCN2	NS	NS	0.41	0.02857	NS	NS	NS	NS
Mx1	6.57	0.05714	6.66	0.02857	NS	NS	NS	NS
SCNA	5.13	0.1143	3.42	0.2	4.17	0.1143	3.49	0.2
STAT1	2.62	0.02857	2.66	0.02857	NS	NS	NS	NS
STAT4	2.44	0.2			0.680	0.2		

transformation of the ovarian surface epithelium [37,38]. The theory suggests that because pregnancy halts ovulation, the ovary is thus protected from any negative effects of ovulation for a time. Another hypothesis suggests that pregnancy clears transformed cells on the surface of the ovary, providing a protective effect [6]. Although investigating the impact of parity on metastasis does not directly address the mechanism by which parity protects against initial development of ovarian cancer, such studies may nevertheless offer insights to this query, as very early events in ovarian cancer progression are thought to include metastasis from the fallopian tube to the surface of the ovary [39].

There is a paucity of studies investigating the effect of parity on metastasis. Furthermore, no previous parity-metastasis study has accounted for specific parity number or controlled for age. Syngeneic allograft mouse models provide the advantage of investigating metastasis in an immunocompetent environment. In the current study, we used a C57Bl/6 syngeneic ID8 MOSE model of parity to investigate how parity number impacts metastatic seeding and growth. We found that multiparity reduces susceptibility to ovarian cancer metastasis. Although not directly tested here, it is conceivable that the effect of multiparity on metastasis contributes to the further reduction in ovarian cancer risk associated with multiple births seen in epidemiologic data [8].

While the above theories and epidemiologic studies address the parity-related effect on incidence of ovarian cancer, recently a single study on ovarian cancer metastasis reported that a parity-related effect on the metastatic niche is a protective factor against metastasis [11]. This study reported that middle-aged multiparous animals injected with a syngeneic C57Bl/6 MOSE cell line (MOSE-LFFLv) developed significantly less tumor burden than the younger virgin animals and that parity was associated with differences in the immune cells in the omental fat band [11]. However, our results differ in several important ways from this published study on parity and ovarian cancer metastasis. Unlike the current report, the published study did not control for parity number or the age of the animals. To this end, it is useful to note that middle-aged C57Bl/6 females undergo persistent estrous and thus do not correlate well

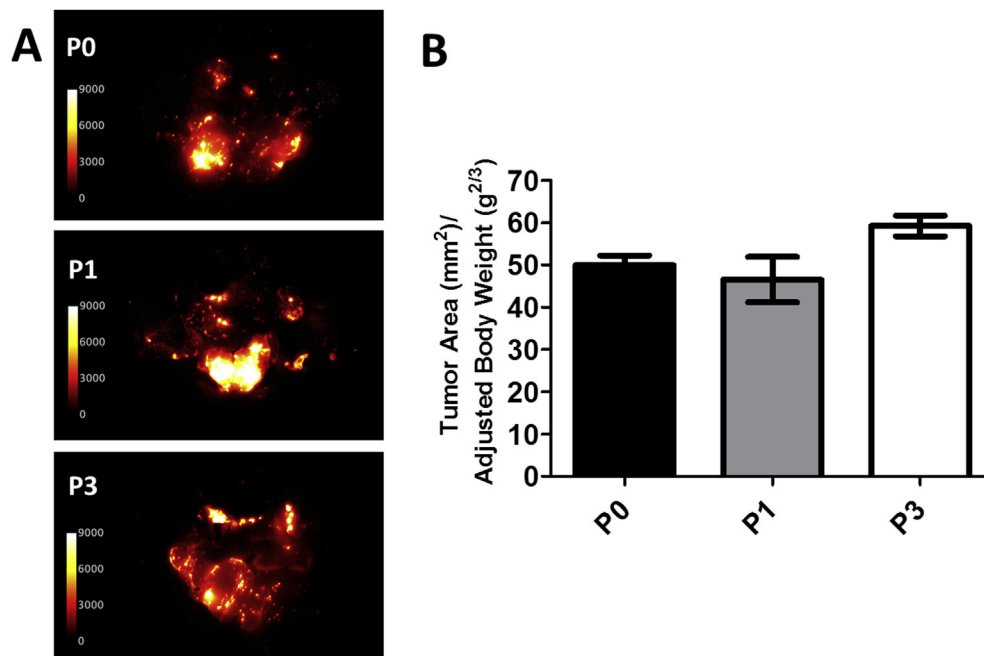


Fig. 4. Impact of parity on abdominal tumor burden *in situ* in aged mice. **A.** Aged mice (20.5-month old) of three parity statuses were injected with 9.6×10^6 ID8-RFP cells. After sacrifice at 8 weeks post IP injection, the abdominal cavity was exposed and imaged. **B.** Tumor area was quantified as described in Materials and Methods. Abdominal tumor area was calculated by dividing the tumor area by the scale-adjusted body weight of each mouse. $N = 5$.

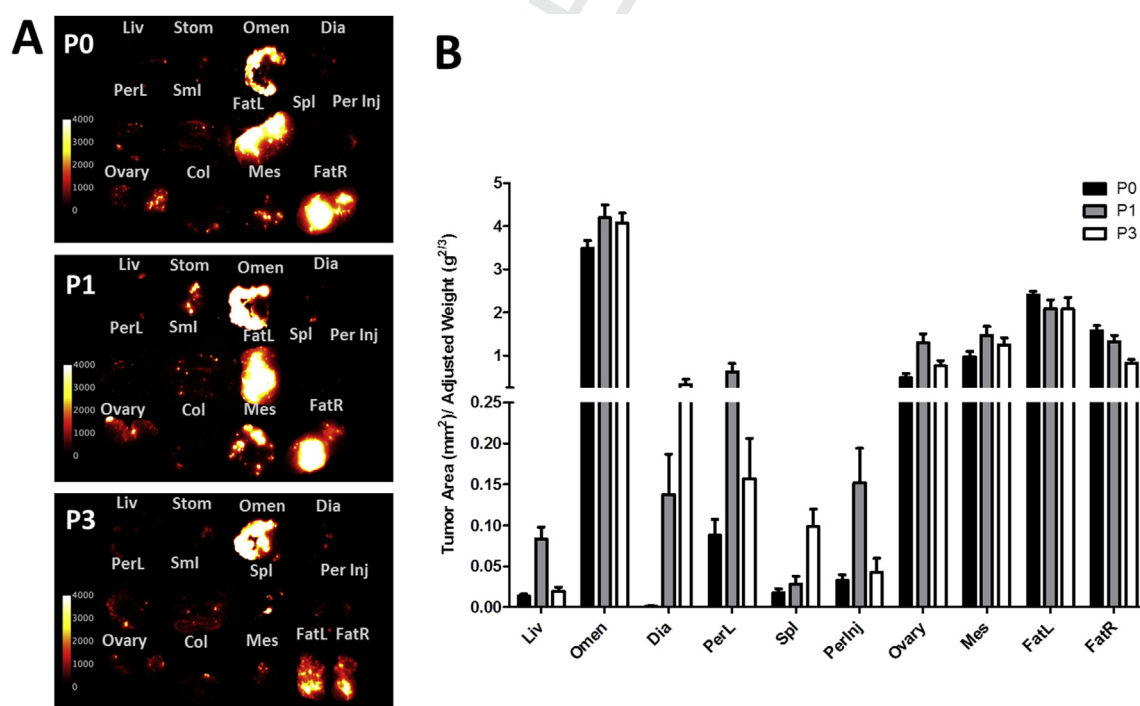


Fig. 5. Evaluation of organ-specific tumor burden in aged P0, P1 and P3 mice. **A.** Individual organs from aged mice were dissected from the peritoneal cavity and imaged. $N = 5$. **B.** Tumor area was quantified to determine the Organ Area Fraction by dividing the tumor area by the adjusted organ weight.

to any human reproductive status [40], as opposed to 20 month animals that are devoid of ovarian follicles [41]. Additionally, we detected no significant difference in metastasis to the omentum in age-matched parous animals injected with ID8 ovarian cancer cells at 8 weeks post injection, but observed significantly reduced metastasis to the gonadal adipose tissue of multiparous mice. Furthermore, our data comparing aged mice (over 20 months)

demonstrate age can be a confounding factor. Given the complexity of the model system, further mechanistic investigation of the impact of parity on ovarian metastasis is warranted.

The multiparous-associated reduction in metastasis was observed specifically in murine gonadal adipose tissue, the largest fat depot in mice. We found that IFN pathways were activated in the gonadal adipose tissue of multiparous animals, which may be

responsible for the observed resilience to metastasis. IFNs are pleiotropic cytokines that activate a number of downstream pathways involved in antiproliferative activity, immunomodulation and host defense [30,31]. Activated IFN pathways may modulate the immune environment in the multiparous gonadal adipose tissue, reducing receptivity to malignant cells. In addition to acting on immune cells, an activated IFN microenvironment could also act directly on cancer cells to hinder their growth in the metastatic niche [30]. Further studies including experiments using an IFN blockade strategy are warranted to elucidate a mechanism by which IFN activation may make the gonadal adipose microenvironment less hospitable for ovarian tumor cells.

While beyond the scope of the current study, there are a number of possible explanations for activated IFN pathways in multiparous animals. Among the many immunological changes that occur during pregnancy in the female reproductive tract, upregulation of IFN-stimulated genes in placental tissue plays an important role in uterine receptivity to implantation [42]. Our data suggests that exposure to multiple pregnancies activates IFN pathways in other areas of the murine gonadal tissue in addition to the endometrium, which may result in a less hospitable environment for intraperitoneal metastasis. Additionally, it has been recently shown that methylome changes in tumor cells can lead to expression of endogenous retroviruses (ERVs), thereby activating type I IFN and resulting in growth inhibition of tumor cells [43]. Pregnancy is known to alter the methylome in breast tissue, and it is conceivable that the reproductive tract is similarly affected [44,45]. Future studies on IFN activation in response to pregnancies in the human ovarian surface epithelium and in peritoneal adipose tissue may provide insight into the parity-related effect on ovarian cancer reported in epidemiologic studies. Specifically, such investigations could inform the “pregnancy-dependent clearance” theory, as it is conceivable ISGs could act as “clearing factors” on the ovarian surface and elsewhere in the peritoneal cavity [6].

The question of how to harness anti-tumorigenic effects of IFNs is a seasoned investigation. For example, IFN α has been utilized for treatment of various illnesses and multiple cancer types including ovarian cancer [46,47]. Unfortunately, there have been mixed results in clinical trials and further attempts to treat ovarian cancer patients with IFN α or IFN γ are not justified [47]. However, alternative approaches such as inducing ISG expression, demonstrated in pre-clinical models that target ovarian cancer cells through IFN activation by DNA methyltransferase inhibitors, warrant additional consideration [43]. Overall, our current study suggests that further investigation into targeting IFN pathways to harness parity-related protective effects for women with metastatic disease may be beneficial.

A recent epidemiologic study suggests that the protective effect of parity decreases with age [36]. McGuire et al. reported that women 50–64 years of age have a 12% risk reduction per full term pregnancy (FTP) and that this percentage drops to 8% in women 65–74 years of age. Women 75 years of age and older were reported to have no benefit per FTP. This data on the reduced parity-related protective effect against ovarian cancer incidence appears to be mirrored in the current aged-parity study of metastasis. Interestingly, in the ID8 allograft model, aged multiparous animals had no resilience to metastasis compared to their primiparous and nulliparous counterparts, suggesting one of the following: that the parity-related protective effect dwindles with age, that age-related effects override the parity-related protection against metastasis, or a combination of both. With this consideration, it is interesting to note that data from our laboratory demonstrate that aged mice are more susceptible to metastasis compared to young mice [48].

In summary, this study of parity and metastasis demonstrates that multiparity provides a protective affect against ovarian cancer

metastasis in the ID8 C57Bl/6 syngeneic allograft model and that this protective effect is lost with age. Our data suggests that a multiparous-associated activation of IFN pathways may provide this protective effect. Future studies are needed to elucidate how multiple pregnancies alter the immune environment in murine models of metastasis and in human tissue, to ultimately explore if further exploitation of IFN pathways is warranted therapeutically, particularly for older women who may have lost any parity-related protective effect once present.

Acknowledgements

This work was supported by Grants RO1CA109545 (MSS) and RO1CA086984 (MSS) from the National Institutes of Health/National Cancer Institute; from the Leo and Anne Albert Charitable Trust (MSS); National Science Foundation Graduate Research Fellowship Program grant DGE-1313583 (EAL).

Conflict of interest

Authors have no conflicts of interest to disclose.

Appendix A. Supplementary data

Supplementary data related to this article can be found at <https://doi.org/10.1016/j.canlet.2017.09.028>.

References

- [1] E. Lengyel, Ovarian cancer development and metastasis, *Am. J. Pathol.* 177 (2010) 1053–1064.
- [2] S. Pradeep, S.W. Kim, S.Y. Wu, M. Nishimura, P. Chaluvaly-Raghavan, T. Miyake, et al., Hematogenous metastasis of ovarian cancer: rethinking mode of spread, *Cancer Cell* 26 (2014) 77–91.
- [3] L.G. Coffman, D. Burgos-Ojeda, R. Wu, K. Cho, S. Bai, R.J. Buckanovich, New models of hematogenous ovarian cancer metastasis demonstrate preferential spread to the ovary and a requirement for the ovary for abdominal dissemination, *Transl. Res.* 175 (2016) 92–102 e102.
- [4] L. Titus-Ernstoff, K. Perez, D.W. Cramer, B.L. Harlow, J.A. Baron, E.R. Greenberg, Menstrual and reproductive factors in relation to ovarian cancer risk, *Br. J. Cancer* 84 (2001) 714–721.
- [5] F. Modugno, R.B. Ness, G.O. Allen, J.M. Schildkraut, F.G. Davis, M.T. Goodman, Oral contraceptive use, reproductive history, and risk of epithelial ovarian cancer in women with and without endometriosis, *Am. J. Obstet. Gynecol.* 191 (2004) 733–740.
- [6] H.O. Adami, M. Lambe, I. Persson, A. Ekblom, H.O. Adami, C.C. Hsieh, et al., Parity, age at first childbirth, and risk of ovarian cancer, *Lancet* 344 (1994) 1250–1254.
- [7] A.S. Whittemore, R. Harris, J. Itnyre, Characteristics relating to ovarian cancer risk: collaborative analysis of 12 US case-control studies. II. Invasive epithelial ovarian cancers in white women. Collaborative Ovarian Cancer Group, *Am. J. Epidemiol.* 136 (1992) 1184–1203.
- [8] K.K. Tsilidis, N.E. Allen, T.J. Key, L. Dossus, A. Lukanova, K. Bakken, et al., Oral contraceptive use and reproductive factors and risk of ovarian cancer in the European Prospective Investigation into Cancer and Nutrition, *Br. J. Cancer* 105 (2011) 1436–1442.
- [9] N. Wentzensen, E.M. Poole, B. Trabert, E. White, A.A. Arslan, A.V. Patel, et al., Ovarian cancer risk factors by histologic subtype: an analysis from the ovarian cancer cohort consortium, *J. Clin. Oncol.* (2016).
- [10] H.A. Risch, L.D. Marrett, G.R. Howe, Parity, contraception, infertility, and the risk of epithelial ovarian cancer, *Am. J. Epidemiol.* 140 (1994) 585–597.
- [11] C.A. Cohen, A.A. Shea, C.L. Heffron, E.M. Schmelz, P.C. Roberts, The parity-associated microenvironmental niche in the omental fat band is refractory to ovarian cancer metastasis, *Cancer Prev. Res.* 6 (2013) 1182–1193.
- [12] K. Flurkey, J.M. Curren, D.E. Harrison, Chapter 20-mouse models in aging research, in: J.G. Fox, M.T. Davisson, F.W. Quimby, S.W. Barthold, C.E. Newcomer, A.L. Smith (Eds.), *The Mouse in Biomedical Research*, second ed., Academic Press, Burlington, 2007, pp. 637–672.
- [13] K.F. Roby, C.C. Taylor, J.P. Sweetwood, Y. Cheng, J.L. Pace, O. Tawfik, et al., Development of a syngeneic mouse model for events related to ovarian cancer, *Carcinogenesis* 21 (2000) 585–591.
- [14] Y. Liu, M.N. Metzinger, K.A. Lewellen, S.N. Cripps, K.D. Carey, E.I. Harper, et al., Obesity contributes to ovarian cancer metastatic success through increased lipogenesis, enhanced vascularity, and decreased infiltration of M1 macrophages, *Cancer Res.* (2015).
- [15] K.A. Lewellen, M.N. Metzinger, Y. Liu, M.S. Stack, Quantitation of intra-peritoneal ovarian cancer metastasis, *J. Vis. Exp. Jove* (2016).

- [16] R-Core-Team, A Language and Environment for Statistical Computing, R Foundation for Statistical Computing, Vienna, Austria, 2014. <http://www.R-project.org/>.
- [17] A.M. Bolger, M. Lohse, B. Usadel, Trimmomatic: a flexible trimmer for Illumina sequence data, *Bioinformatics* 30 (2014) 2114–2120.
- [18] S. Andrews, FastQC, Babraham Bioinformatics, Babraham Institute, 2014. <http://www.bioinformatics.babraham.ac.uk/projects/fastqc>.
- [19] F. Cunningham, M.R. Amode, D. Barrell, K. Beal, K. Billis, S. Brent, et al., Ensembl 2015, *Nucleic Acids Res.* 43 (2015) D662–D669.
- [20] C. Trapnell, L. Pachter, S.L. Salzberg, TopHat: discovering splice junctions with RNA-Seq, *Bioinformatics* 25 (2009) 1105–1111.
- [21] B. Langmead, S.L. Salzberg, Fast gapped-read alignment with Bowtie 2, *Nat. Methods* 9 (2012) 357–359.
- [22] H. Li, B. Handsaker, A. Wysoker, T. Fennell, J. Ruan, N. Homer, et al., S. Genome Project Data Processing, The sequence alignment/map format and SAMtools, *Bioinformatics* 25 (2009) 2078–2079.
- [23] S. Anders, P.T. Pyl, W. Huber, HTSeq—a Python framework to work with high-throughput sequencing data, *Bioinformatics* 31 (2015) 166–169.
- [24] D. Wheeler, How to use DESeq to Analyse RNAseq Data, David Wheeler Lab, 2013. <https://dwheelerau.com/2013/2004/2015/how-to-use-deseq-to-analyse-rnaseq-data/>.
- [25] D.J. McCarthy, Y. Chen, G.K. Smyth, Differential expression analysis of multi-factor RNA-Seq experiments with respect to biological variation, *Nucleic Acids Res.* 40 (2012) 4288–4297.
- [26] M.D. Robinson, D.J. McCarthy, G.K. Smyth, edgeR: a Bioconductor package for differential expression analysis of digital gene expression data, *Bioinformatics* 26 (2010) 139–140.
- [27] M.D. Robinson, G.K. Smyth, Moderated statistical tests for assessing differences in tag abundance, *Bioinformatics* 23 (2007) 2881–2887.
- [28] M.D. Robinson, G.K. Smyth, Small-sample estimation of negative binomial dispersion, with applications to SAGE data, *Biostatistics* 9 (2008) 321–332.
- [29] R.J. Kinsella, A. Kahari, S. Haider, J. Zamora, G. Proctor, G. Spudich, et al., Ensembl BioMart: a hub for data retrieval across taxonomic space, *Database (Oxford)* 2011 (2011) bar030.
- [30] L.C. Platanias, Mechanisms of type-I- and type-II-interferon-mediated signalling, *Nat. Rev. Immunol.* 5 (2005) 375–386.
- [31] L.B. Ivashkiv, L.T. Donlin, Regulation of type I interferon responses, *Nat. Rev. Immunol.* 14 (2014) 36–49.
- [32] K. Honda, H. Yanai, H. Negishi, M. Asagiri, M. Sato, T. Mizutani, et al., IRF-7 is the master regulator of type-I interferon-dependent immune responses, *Nature* 434 (2005) 772–777.
- [33] A. Kroger, M. Koster, K. Schroeder, H. Hauser, P.P. Mueller, Activities of IRF-1, J. Interferon Cytokine Res. 22 (2002) 5–14.
- [34] D.J. Vestal, J.A. Jeyaratnam, The guanylate-binding proteins: emerging insights into the biochemical properties and functions of this family of large interferon-induced guanosine triphosphatase, *J. Interferon Cytokine Res.* 31 (2011) 89–97.
- [35] S. LeibundGut-Landmann, J.M. Waldburger, M. Krawczyk, L.A. Otten, T. Suter, A. Fontana, et al., Mini-review: specificity and expression of CIITA, the master regulator of MHC class II genes, *Eur. J. Immunol.* 34 (2004) 1513–1525.
- [36] V. McGuire, P. Hartge, L.M. Liao, R. Sinha, L. Bernstein, A.J. Canchola, et al., Parity and oral contraceptive use in relation to ovarian cancer risk in older women, *Cancer Epidemiol. Biomarkers Prev. Publ. Am. Assoc. Cancer Res. Cosponsored Am. Soc. Prev. Oncol.* 25 (2016) 1059–1063.
- [37] M.F. Fathalla, Incessant ovulation and ovarian cancer – a hypothesis revisited, *Facts Views Vis. Obgyn.* 5 (2013) 292–297.
- [38] M.F. Fathalla, Incessant ovulation—a factor in ovarian neoplasia? *Lancet* 2 (1971) 163.
- [39] R. Vang, M. Shih Ie, R.J. Kurman, Fallopian tube precursors of ovarian low- and high-grade serous neoplasms, *Histopathology* 62 (2013) 44–58.
- [40] J.F. Nelson, L.S. Felicio, P.K. Randall, C. Sims, C.E. Finch, A longitudinal study of estrous cyclicity in aging C57BL/6J mice: I. Cycle frequency, length and vaginal cytology, *Biol. Reprod.* 27 (1982) 327–339.
- [41] G.I. Perez, R. Robles, C.M. Knudson, J.A. Flaws, S.J. Korsmeyer, J.L. Tilly, Prolongation of ovarian lifespan into advanced chronological age by Bax-deficiency, *Nat. Genet.* 21 (1999) 200–203.
- [42] F.W. Bazer, Part J: placental interferons, implantation and pregnancy, in: O.S. Gérard Chauat, Nathalie Lédée (Eds.), *Immunology of Pregnancy*, Bentham Science Publishers, Oak Park, IL, 2013, pp. 397–421.
- [43] K.B. Chiappinelli, P.L. Strissel, A. Desrichard, H. Li, C. Henke, B. Akman, et al., Inhibiting DNA methylation causes an interferon response in cancer via dsRNA including endogenous retroviruses, *Cell* 162 (2015) 974–986.
- [44] S. Ghosh, F. Gu, C.M. Wang, C.L. Lin, J. Liu, H. Wang, et al., Genome-wide DNA methylation profiling reveals parity-associated hypermethylation of FOXA1, *Breast Cancer Res. Treat.* 147 (2014) 653–659.
- [45] T.A. Katz, S.G. Liao, V.J. Palmieri, R.K. Dearth, T.N. Pathiraja, Z. Huo, et al., Targeted DNA methylation screen in the mouse mammary genome reveals a parity-induced hypermethylation of Igf1r that persists long after parturition, *Cancer Prev. Res.* 8 (2015) 1000–1009.
- [46] M. Ferrantini, I. Capone, F. Belardelli, Interferon-alpha and cancer: mechanisms of action and new perspectives of clinical use, *Biochimie* 89 (2007) 884–893.
- [47] A.O. Lawal, A. Musekiwa, L. Grobler, Interferon after surgery for women with advanced (Stage II-IV) epithelial ovarian cancer, *Cochrane Database Syst. Rev.* (2013) CD009620.
- [48] E.A. Loughran, A.K. Leonard, R.C. Phan, M.G. Yemc, T. Hilliard, M. Asem, et al., Aging increases susceptibility to ovarian cancer metastasis in murine allograft models and alters immune composition in peritoneal adipose tissue, (Submitted).